Using Cramér-Rao Theory For SAR Waveform Design

Robert Linnehan[a], David Brady[b], John Schindler[c], Leonid Perlovsky[a], Muralidhar Rangaswamy[a]
[a] Air Force Research Laboratory, Hanscom AFB, MA
[b] Northeastern University, Boston, MA
[c] Anteon Corporation, Hanscom AFB, MA
E-mail: robert.linnehan2@hanscom.af.mil, Tel: (781)377-1732, Fax: (781)377-8984

ABSTRACT

This paper applies Cramér-Rao theory to synthetic aperture radar (SAR) in order to establish optimal performance bounds on target parameter estimation. The Cramèr-Rao bound (CRB) establishes a lower bound on the error variance of unbiased or asymptotically efficient parameter estimates [8]. Bounds on the estimation of various target parameters are developed, and the extension to multistatic SAR (MSAR) is considered.

1. *INTRODUCTION*

A standard one-pass SAR image can be regarded as the estimation of the 2-dimensional position and complex scattering coefficients at fixed points on the ground. CRBs applied to scatterer position and reflectivity offer the smallest possible error variances on those estimates independently from the method of estimation. The bounds can be used to enhance system design by optimizing performance with respect to system parameters. In [1] we considered the CRB for scatterer reflectivity with the assumption that the sensor position is known with respect to all scatterers on the ground, the only source of random error being measurement noise. By creating a scattering model with a limited number of scatterers, bounds were derived for all reflectivities simultaneously. We now derive CRBs for the joint estimation of the 3-dimensional features, as well as reflectivities. In this case all scatterer positions in range, cross-range and elevation are considered unknown. The CRBs are in general dependent on the scatterer parameter values, the radar parameters and the relative position of the radar to the scatterers. To estimate scatterer heights, vertical excursion of the radar platform is required when forming the synthetic aperture. The development is extended to multistatic SAR where a single radar is transmitting and several radars are receiving.

Previous literature describes the use of CRBs for SAR parametric estimation techniques. In [9], maximum likelihood estimation of interferometric SAR parameters are compared with derived bounds. In [3], CRBs are used to evaluate spectral estimation methods applied to curvilinear SAR. However, we are offering a more general approach to the analytical capabilities of Cramér-Rao theory for any aperture, scattering model or radar properties that might answer the questions posed by SAR engineers. For instance, given a simulated scattering model, what range, azimuth and elevation should the positions of the synthetic array be located if the goal is to minimize the error on height estimation? In the multistatic case, how many receivers are needed and where should they be positioned in order to achieve some minimum variance on the complex reflectivities? The simplicity of Cramér-Rao theory allows for, what would otherwise be very computationally complex, a convenient means to optimize SAR and MSAR waveforms. It is our intention to provide those in the SAR research community a tool to efficiently evaluate and optimize existing or developmental signal processing algorithms.

2. *THE SCATTERING & SIGNAL MODELS*

The scattering model consists of a finite number of scatterers located within a square grid of cells that are placed on the nominal ground level at ground range $y = 0\ m$ and cross-range $x = 0\ m$. Although the bounds for all scatterers are computed, our analysis is on one scatterer (hereafter called the target) located at the center of this grid given its bounds will reflect the worst case. Figure 1 shows scatterer n located at cross-range x_n, range y_n and height h_n, with the radar located at x_{ac}, y_{ac} and h_{ac} as a function of time t.

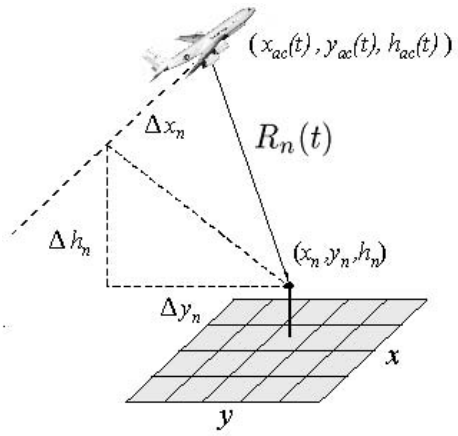

Fig. 1. Dimensional description

The signal model, over the observation time on the array, is [1]

$$s(t) = \sum_{n=1}^{N} a_n A_n(t), \tag{1}$$

$$A_n(t) = \sum_{k=1}^{N_f} \frac{1}{R_n^2(t)}\, e^{j\omega_k (t - \frac{2R_n(t)}{c})}, \tag{2}$$

0-7803-8882-8/05/$20.00 (C) 2005 IEEE

Report Documentation Page

Form Approved
OMB No. 0704-0188

Public reporting burden for the collection of information is estimated to average 1 hour per response, including the time for reviewing instructions, searching existing data sources, gathering and maintaining the data needed, and completing and reviewing the collection of information. Send comments regarding this burden estimate or any other aspect of this collection of information, including suggestions for reducing this burden, to Washington Headquarters Services, Directorate for Information Operations and Reports, 1215 Jefferson Davis Highway, Suite 1204, Arlington VA 22202-4302. Respondents should be aware that notwithstanding any other provision of law, no person shall be subject to a penalty for failing to comply with a collection of information if it does not display a currently valid OMB control number.

1. REPORT DATE	2. REPORT TYPE	3. DATES COVERED
01 MAY 2005	**N/A**	**-**

4. TITLE AND SUBTITLE	5a. CONTRACT NUMBER
Using Cram´er-Rao Theory For SAR Waveform Design	5b. GRANT NUMBER
	5c. PROGRAM ELEMENT NUMBER
6. AUTHOR(S)	5d. PROJECT NUMBER
	5e. TASK NUMBER
	5f. WORK UNIT NUMBER
7. PERFORMING ORGANIZATION NAME(S) AND ADDRESS(ES) **Air Force Research Laboratory, Hanscom AFB, MA**	8. PERFORMING ORGANIZATION REPORT NUMBER
9. SPONSORING/MONITORING AGENCY NAME(S) AND ADDRESS(ES)	10. SPONSOR/MONITOR'S ACRONYM(S)
	11. SPONSOR/MONITOR'S REPORT NUMBER(S)

12. DISTRIBUTION/AVAILABILITY STATEMENT
Approved for public release, distribution unlimited

13. SUPPLEMENTARY NOTES
See also ADM002017. Proceedings of the 2005 IEEE International Radar Conference Record Held in Arlington, Virginia on May 9-12, 2005. U.S. Government or Federal Purpose Rights License., The original document contains color images.

14. ABSTRACT

15. SUBJECT TERMS

16. SECURITY CLASSIFICATION OF:			17. LIMITATION OF ABSTRACT	18. NUMBER OF PAGES	19a. NAME OF RESPONSIBLE PERSON
a. REPORT	b. ABSTRACT	c. THIS PAGE			
unclassified	**unclassified**	**unclassified**	**UU**	**5**	

where the summation in equation (1) is over all scatterers $n = 1 \ldots N$ in the grid, and the summation on k in equation (2) represents the inclusion of frequency samples ω_k, $k = 1 \ldots N_f$, from the passband linear FM pulse. R_n and a_n are the slant range and complex reflectivity of scatterer n, respectively, and c is the speed of light. The slant range at time t may be expressed as

$$R_n(t) = \sqrt{\Delta x_n^2(t) + \Delta y_n^2(t) + \Delta h_n^2(t)}, \tag{3}$$

where $\Delta h_n(t) = (h_n - h_{ac}(t))$. Other differential lengths are defined similarly and are described in Figure 1.

The received signal model is,

$$r(t) = s(t) + n(t), \ t = 1, \ldots T, \tag{4}$$

where $n(t)$ is a stationary white, circular Gaussian random process.

3. *CRB DERIVATION*

In this section we define θ to be the vector of real parameters to be estimated, in no particular order. For each target or scatterer, this includes the two quadrature reflectivity components, and the three positional components. Due to the complex white noise model, a sufficient statistic for θ is given by $S = \sum_t \mathrm{Re}\left\{(r(t) - \frac{1}{2}s(t))s^*(t)\right\}$, which is Gaussian with mean $\frac{1}{2}\sum_t |s(t)|^2$ and variance $\sigma_0^2 \sum_t |s(t)|^2$. Here, σ_0^2 is the noise variance in each quadrature component at time t. It is easy to show that the ij^{th} component of the Fisher Information Matrix (FIM) is given by

$$\begin{aligned}\mathbf{J}_{ij} &= \frac{1}{2\sum_t |s(t)|^2}\left(\sum_t \frac{\partial}{\partial\theta_i}|s(t)|^2\right)\left(\sum_t \frac{\partial}{\partial\theta_j}|s(t)|^2\right) \times \\ &\times \left(\frac{1}{\sum_t |s(t)|^2} + \frac{1}{2\sigma_0^2}\right)\end{aligned} \tag{5}$$

Bounds on the variance of unbiased estimators for θ depend on the first-order partial derivatives of the squared signal magnitude. When θ_i belongs to the k^{th} scatterer,

$$\frac{\partial}{\partial\theta_i}|s(t)|^2 = 2s^*(t)\frac{\partial}{\partial\theta_i}\left(a_k A_k(t)\right)$$

4. *NUMERICAL RESULTS*

In typical SAR imaging, the reflectivity of a large ground area is estimated to include a large number of scatterers. However, when performing CRB analysis it is necessary to limit the number of scatterers in the simulated model to avoid computational complexity. The size of the grid and the density of scatterers should be enough to reproduce the effects of an infinitely large scattering area around the target, but small enough to limit the number of computations and the size of the matrix $\mathbf{J}$ to be inverted. The influence from surrounding scatterers decreases relative to their distance from the target. In [1] we showed the CRB for the target reaches a maximum value when the single side dimension of a square grid of scatterers reaches approximately 14 m (given the target scatterer is at the center of the grid). The scatterers are separated by a distance of $1m$ from each other and the radar parameters used in this experiment are as follows: center frequency $f_c = 450\ MHz$, bandwidth $B = 60\ MHz$, and synthetic aperture length $L = 5000\ m$. In Figure 2 one can see that scatterers placed beyond a 14 $m \times 14\ m$ square grid have little impact on estimating the target reflectivity for the system considered here.

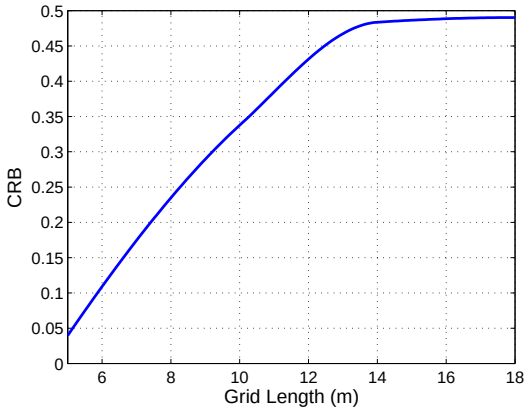

Fig. 2. CRB for a_1 vs. grid size

Other considerations to limit the number of computations are the pulse repetition frequency (PRF) and the frequency sampling rate (FSR) of the linear FM pulse should be limited. The PRF and FSR are minimized with the assurance that quasi-grating lobes in the azimuth and ground range dimensions, respectively, are physically beyond the limits of the scattering model. Figure 3 shows the magnitude response of the white noise matched filter in the azimuth and range dimensions (given the operational parameters mentioned above) with a PRF of 1 $pulse/sec$ and a frequency sampling period of 10 MHz. It is evident that the first quasi-grating lobes (indicated by the arrows) are beyond the distance from the target ($\sim 7\ m$) required to emulate an infinitely large area arou dimensions.

The complex reflectivities of the scatterers are randomly generated and represented as

$$a_n = \alpha + j\beta \tag{6}$$

where

$$\alpha, \beta \sim \mathcal{N}(0, \sigma_a^2). \tag{7}$$

Assuming the components α and β are statistically independent Gaussian random variables, the magnitude of a_n will be Rayleigh distributed [7]. The mean and variance of the scatterers (clutter) are respectively,

$$\begin{aligned}\mu_c &= \sigma_a\sqrt{\tfrac{\pi}{2}} \\ \sigma_c^2 &= (2 - \tfrac{\pi}{2})\sigma_a^2\end{aligned} \tag{8}$$

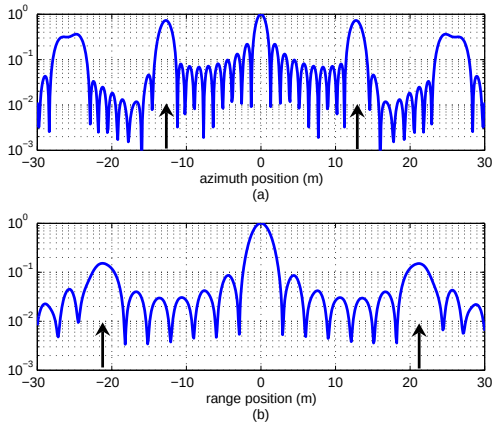

Fig. 3. Magnitude response in x and y dimensions

We define the target to have a similar complex reflectivity distributed as (7) but with a different variance σ_t^2. The signal to clutter ratio (SCR) can be computed as,

$$\text{SCR} = \frac{\mu_t^2}{\mu_c^2} = \frac{\sigma_t^2}{\sigma_a^2} \tag{9}$$

The simulations described in this paper have an SCR of 0 dB since we are denoting the target as an ordinary scatterer to be estimated.

It is intuitively expected that height estimation is an ill-posed problem for standard SAR [1]. Allowing some vertical excursion in forming the aperture provides additional information and conditions the matrix $\mathbf{J}$. The Fisher information matrix for one scatterer can be written as,

$$\mathbf{J} = \frac{4|a_1|^2}{c^2\sigma_0^2} \sum_{t=1}^{T} \sum_{k=1}^{N_f}$$

$$\begin{pmatrix} \frac{\Delta x_1^2(t)\omega_k^2}{R_1^6(t)} & \frac{\Delta x_1(t)\Delta y_1(t)\omega_k^2}{R_1^6(t)} & \frac{\Delta x_1(t)\Delta h_1(t)\omega_k^2}{R_1^6(t)} & \frac{c\,\Delta x_1(t)\omega_k}{2a_1^* R_1^5(t)} \\ \frac{\Delta y_1(t)\Delta x_1(t)\omega_k^2}{R_1^6(t)} & \frac{\Delta y_1^2(t)\omega_k^2}{R_1^6(t)} & \frac{\Delta y_1(t)\Delta h_1(t)\omega_k^2}{R_1^6(t)} & \frac{c\,\Delta y_1(t)\omega_k}{2a_1^* R_1^5(t)} \\ \frac{\Delta h_1(t)\Delta x_1(t)\omega_k^2}{R_1^6(t)} & \frac{\Delta h_1(t)\Delta y_1(t)\omega_k^2}{R_1^6(t)} & \frac{\Delta h_1^2(t)\omega_k^2}{R_1^6(t)} & \frac{c\,\Delta h_1(t)\omega_k}{2a_1^* R_1^5(t)} \\ \frac{c\,\Delta x_1(t)\omega_k}{2a_1 R_1^5(t)} & \frac{c\,\Delta y_1(t)\omega_k}{2a_1 R_1^5(t)} & \frac{c\,\Delta h_1(t)\omega_k}{2a_1 R_1^5(t)} & \frac{c^2}{4|a_1|^2 R_1^4(t)} \end{pmatrix}. \tag{10}$$

The diagonal of $\mathbf{J}^{-1}$ will yield bounds for the scatterer parameter estimates. If multiple scatterers are included in the model, the diagonal elements of the center 4 x 4 block diagonal matrix of $\mathbf{J}^{-1}$ correspond to the bounds of the target.

Computations were performed on a 7×7 cell grid (49 scatterers) with the target scatterer having reflectivity a_1 at the center cell. The cells are arranged so that the cell centers are 2.5 meters apart. The position of the scatterer within each cell is random, uniformly distributed in range and cross-range. The heights of all the scatterers are also random, Gaussian distributed with mean height $3\ m$ and standard deviation $\sigma_h = 1$. An illustration of one scattering realization is seen in Figure 4. It is possible that scatterers, for a given realization, can be located below the nominal ground level.

A simulated experiment examines the CRB for an aircraft with a sinusoidal flight path. There are a total number of 100 pulses over the aperture. The aircraft is moving at 112 m/s (218 knots) with spacial frequency $\frac{1}{5000}\frac{cycle}{meters}$ and amplitude $300\ m$. The radar is restricted to a plane in the x and h dimensions at a ground range of 3000 m from the target (Δy is not a function of time). The center cell is located at 0 m in azimuth and 0 m in range. A simplification made in the simulations is that the scatterer reflectivities do not change with the radar look-angle. Cramér Rao bounds were averaged for fifty scattering model realizations. Figure 5a shows the planar position of the aircraft in azimuth and elevation. The corresponding improvements in the average bounds as the radar aperture is formed are seen in Figure 5b. (the bounds are not computed for the first several array positions because insufficient data results in poorly conditioned matrices. Constant values were assigned to the plot in Figure 5b when the aircraft's position in azimuth is less than -3500 m relative to the target.)

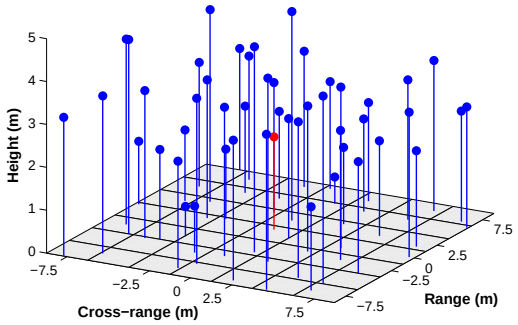

Fig. 4. Scattering model realization

5. *MULTISTATIC SAR*

Multistatic synthetic aperture radar is a developing area of study that can improve the vulnerability to physical or electronic countermeasures [10]. MSAR can also improve the 3-dimensional imaging quality and integration time relative to the monostatic case [11]. Although the topic warrants a lengthy discussion, our goal in this paper is to introduce Cramér Rao theory on a simplified model of MSAR in anticipation of more detailed publications.

The MSAR system under consideration has one aircraft radar acting as a transmitter and receiver, while additional aircrafts act as a receivers only. Similar to the monostatic case, we are assuming there are no phase variations from the scatterers as a function of look angle for any of the receivers. Furthermore, the noise power σ_0^2 is assumed equal for all receivers. Finally, the method of communication between the

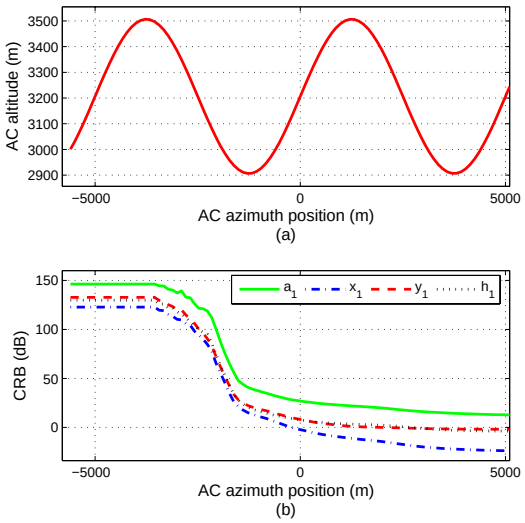

Fig. 5. (a) Radar position (b) Improvement of CRBs as the synthetic aperture forms

radar platforms or to a common ground station, or how the data is fused is not considered in this discussion. The combined CRBs of the multistatic system offer a measure of improvement in parameter estimation over monostatic SAR.

The received signal, given the simplifications mentioned above, for the multistatic case of $m = 1 \dots M$ receivers can be written as,

$$r(t) = \sum_{m=1}^{M} \sum_{n=1}^{N} \frac{a_n}{R_{n1}(t) R_{nm}(t)} \, e^{j\omega_k (t - \frac{R_{n1}(t) + R_{nm}(t)}{c})} + n_m(t), \tag{11}$$

where R_{n1} is the slant range from the transmitter to scatter n, and R_{nm} is the range from scatterer n to receiver m, $m = 1$ being the transmitter/receiver radar. The Fisher information matrix can be carried out in a similar fashion to the monostatic case, and the parameter CRBs are located along the diagonal of $\mathbf{J}^{-1}$.

The following simulations provide some insight into the possible improvement with MSAR. The radars assumes the same operational parameters as the radar in the previous simulation.. An illustration of the set-up is seen in Figure 6. The flight paths are located in a two-dimensional plane and the arrow indicates the aircraft headings. The number indicates the order in which the receivers are plotted for the various parameter bounds in Figure 7. The solid line in each of the four graphs represents the monostatic case, the dotted line represents the addition of receiver 2 (bistatic SAR), and the remaining lines represent the addition of receivers 3 and 4. The abscissa indicates the pulse number transmitted and subsequently received by all four radars. Note the marked improvement in the bound in the y dimension, for instance, when the second receiver is included in the processing.

Another MSAR example employs a single transmit-only

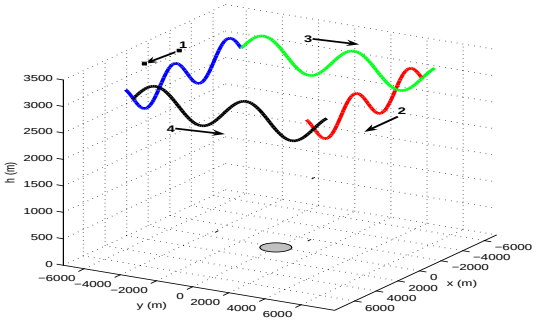

Fig. 6. Multistatic SAR formation

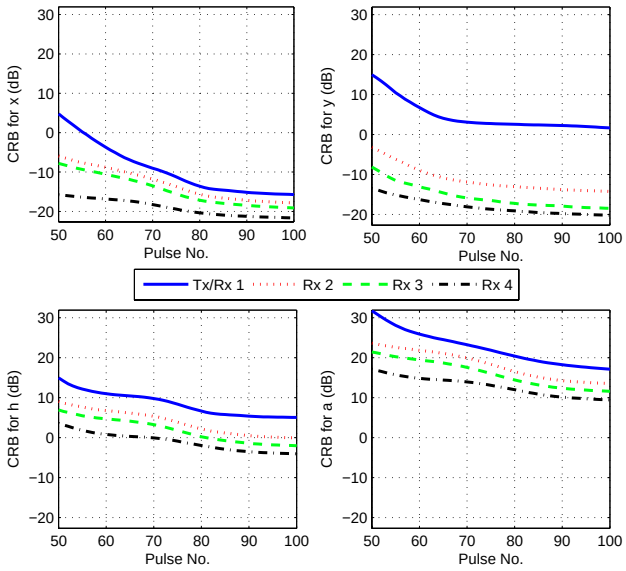

Fig. 7. CRBs for Receivers in Figure 6

platform that is moving in a linear path offset from the target by 10,000 m with a velocity of 175 m/s. Four receiving radars move in sinusoidal paths at 50 m/s around the target area. The receivers in are labelled Rx2, Rx3, Rx4, and Rx5 as indicated in Figure 8. The results of the simulation are seen in Figure 9.

6. *CONCLUSION*

We have developed Cramér-Rao bounds for SAR and MSAR. The bounds can be used for optimal system design, for cooperative control of multiple platforms, or serve as a reference for comparison with practical processing algorithms. Particularly we showed that by including aperture in the vertical dimension, it is possible to jointly estimate 3-D scatterer features with single-pass SAR. We have also demonstrated the potential improvement of multistatic systems. Using these methods, optimization on the performance of SAR waveforms or integrated multiple platforms is possible.

Further work in this area will incorporate the use of improved, more realistic scattering models. We will detail a

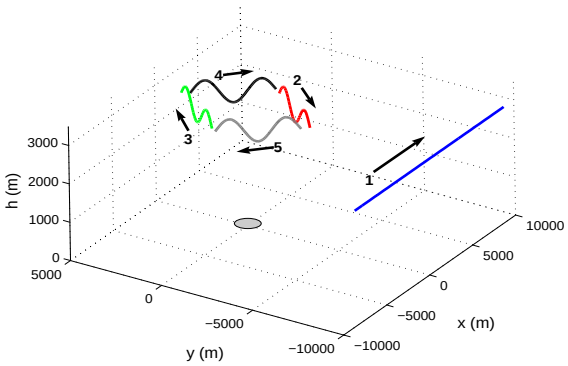

Fig. 8. Multistatic SAR formation

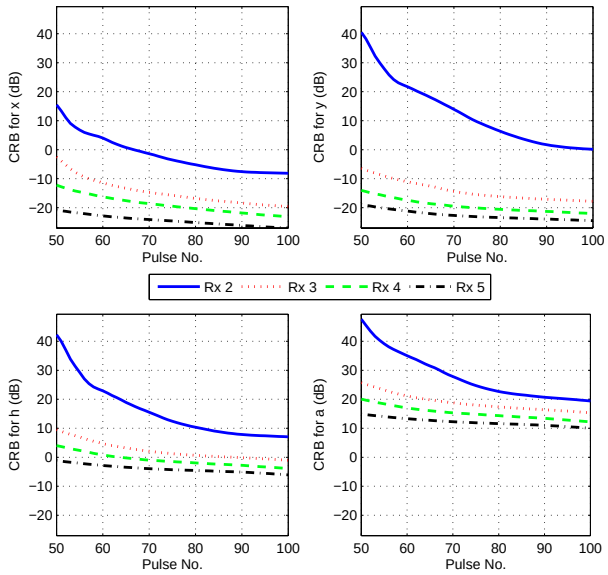

Fig. 9. CRBs for Receivers in Figure 8

method to adaptively optimize the waveform as the synthetic aperture is formed. Finally, we will address cooperative control and optimization of multistatic SAR with respect to target parameter estimates.

AKNOWLEDGEMENT

This work was supported by the Air Force Office of Scientific Research (AFOSR).

REFERENCES

[1] R. Linnehan, J. Schindler, L. Perlovsky, M. Rangaswamy, D. Brady,*Phenomenology-based waveform design using Cramèr Rao theory*, IEE proceedings Waveform Diversity and Design, 2004

[2] H. Cramér, *Mathematical Methods of Statistics*, Princeton University Press, Princeton, NJ, 1946.

[3] J. Li, Z. Bi, Z.-SLiu, K. Knaell,"Use of curvilinear SAR for three-dimensional target feature extraction", IEE Proceedings - Radar, Sonar and Navigation, volume 144, issue 5, pp. 275 - 283 (1997)

[4] A. Papoulis, *Probability, Random Variables and Stochastic Processes*, McGraw-Hill, New York, NY, 1965.

[5] L.I. Perlovsky, *Neural Networks and Intellect: Using Model-Based Concepts*, Oxford University Press, New York, NY. 2001.

[6] L.I. Perlovsky, C.P. Plum, P.R. Franchi, E.J. Tichovolsky, D.S. Choi, B. Weijers. Einsteinian Neural Network for Spectrum Estimation. Neural Networks, 10(9), 1997, pp.1541-46.

[7] C.W. Helstrom, *Elements of Signal Detection and Estimation*, Prentice Hall, Englewood Cliffs, NJ, 1995.

[8] L.L. Scharf, *Statistical Signal Processing*, Addison-Wesley, Reading, MA, 1991.

[9] M.S. Seymour, I.G. Cumming,"Maximum likelihood estimation for SAR interferometry", Geoscience and Remote Sensing Symposium, 1994 , pp. 2272 - 2275.

[10] A.M. Horne, G. Yates, "Bistatic synthetic aperture radar", Radar 2002 Meeting, October 15, 2002, pp. 6 - 10.

[11] M.J.B. Kassem, A. Khenchaf, "Bistatic mapping radar BISAR", OCEANS. MTS/IEEE Conference Proceedings Meeting, Vol.5, September 22, 2003, pp. 2754 - P2760.